Journal of Power Sources, 42 (1993) 365–376

Influence of the operating conditions and of the ageing upon the electrochemical performance of a phosphoric acid fuel cell

V. Alderucci, V. Recupero, E. Passalacqua, R. di Leonardo, M. Laganà and N. Giordano

CNR Institute for Transformation and Storage of Energy, Salita S. Lucia sopra Contesse 39, 98126 S. Lucia, Messina (Italy)

(Received August 5, 1992; accepted in revised form November 10, 1992)

Abstract

As a key step towards the development of a prototype of a 1 kW phosphoric acid fuel cell at the CNR-TAE Institute, the first made in Europe based on an 'in-house' know-how, tests in a subscale monocell station have been performed. The main objective of these studies was to establish the optimum operating conditions as well as to determine the effects of ageing on the cell performance. Prolonged tests totalling more than 40 000 h operations in a monocell have provided useful information to select and scale up the range of optimal operating conditions for the 1-kW stack. This paper illustrates the main findings for phosphoric acid management, humidifier temperature of gases and cell working current density. The endurance tests indicated that the most predominant mechanism of decay is the PTFE–carbon electrostatic corrosion, its extent being strongly a function of cell potential. Performance losses due to platinum catalyst dissolution and/or sintering have been estimated to be in the order of 2mV/1000 h.

Introduction

Among the different types of fuel cells designed for commercial applications, the phosphoric acid fuel cell (PAFC) is the most mature in terms of technological advancement and readiness for commercialization. The major driving force for its dominant position has been the widespread consensus that it, alone among the lower temperature fuel cells, shows relative tolerance to reformed hydrocarbon fuels.

In the USA, the Department of Energy, Electric Power Research Institute, Gas Research Institute, International Fuel Cell (IFC) and others have been pursuing the development of 0.2 to 11 MWe power plants for electric utility and industrial markets. In Japan a project to develop PAFC of the 200-kW power class has been in progress since 1986. This five-year programme is aimed to develop an 'on-site' fuel cell which would permit power units to be installed in various kinds of power demand region [1].

In Europe it was recognized that the technology gap with the USA and Japan was too large to bridge. However, since the present cost of an installed system remains very high (US $2500 per kW with breakeven cost at around US $1300 per kW [2]) a large area of interest still remains, in which the improvements in stack engineering

0378-7753/93/$6.00

and crucial components such as the electrodes, electrocatalysts, bipolar plates and electrolyte matrix play important roles.

The efforts of the Commission of the European Communities have addressed the potentially promising area of stack engineering and component improvement, supporting and coordinating the activities mainly in the Netherlands and Italy. In the Netherlands Kinetics Technology International (KTI), cosponsored by the CEC and the National Government, started a demonstration programme with 25- and 300-kW units [3]. In Italy two options have been selected: (i) to incorporate non-European fuel cell stack technology into European multi-kW fuel cell units; the biggest plant, incorporating two IFC (USA) 675-kW fuel cell stacks, has been designed and built by Ansaldo and will be installed by 1992 in the Milan Municipal Energy Authority grid; (ii) to develop 'in-house' small-scale fuel cell stacks integrated with a fuel processor unit. This has been accomplished by the National Council of Research (CNR) Institute for Transformation and Storage of Energy (TAE) of Messina (Italy) in the framework of a national programme (Progetto Volta). The 1-kW unit, completed in the first months of 1991, is now under test, after an accumulated experience of more than 40 000 h operations in subscale monocell tests devoted to materials and engineering development. Presently, CNR-TAE is the only producer of PAFC stacks in Europe [3]. Plans to expand these activities are now under scrutiny.

The key steps supporting these activities have been: (i) development of a catalyst having a high platinum surface area and high stability in H_3PO_4 [4–7]; (ii) preparation of electrodes with optimized morphology and able to operate at high current densities [8–11], and (iii) development of matrices prepared either by rolling or screen-printing techniques having low ionic resistance and high electrolyte retention capacity.

Material's improvements have been finalized in order to select working conditions (temperature, flow rates, current density) at which the effects on the cell performance and stability of carbon corrosion, platinum sintering and/or dissolution and ohmic losses are minimized.

This paper summarizes the results from subscale monocell tests. It focuses on experiments that establish limits and benefits of operating conditions such as cell current densities, fuel humidifier temperature, and phosphoric acid management. This presentation is limited to few selected runs choosen to show how combination of higher surface area electrocatalyst and improved morphological absorptive capacities of the electrodes has allowed progress in current densities, and therefore, in attainable power density. Currently steady-power densities in the order of 150–175 mW cm^{-2} are obtained in monocells at atmospheric pressure, 180 °C (98% H_3PO_4), close to the state-of-the-art performance (200–210 mW cm^{-2}) [12, 13]. Some preliminary considerations on the effects of ageing on performance are also reported.

Experimental test plant

Figure 1 shows a schematic of the monocell test stand which was designed with the highest flexibility in the working conditions. The fuel is supplied to the monocell from a H_2 tank (1), with provisions made for sending inert gases automatically (2, 3) (N_2 to the cathode and CO_2 to the anode), in case of failure of the H_2 flow. The air is supplied by a compressor (4) connected to a high-pressure pneumatic valve. An additional generator for auxiliaries is used in case of incidental or accidental power-cuts. The water-vapour content in the fuel and/or in the oxidant is regulated by an humidification system (5) placed before the monocell. Electrical plates inside the monocell box are used to heat the cell; absolute and differential pressure trans-

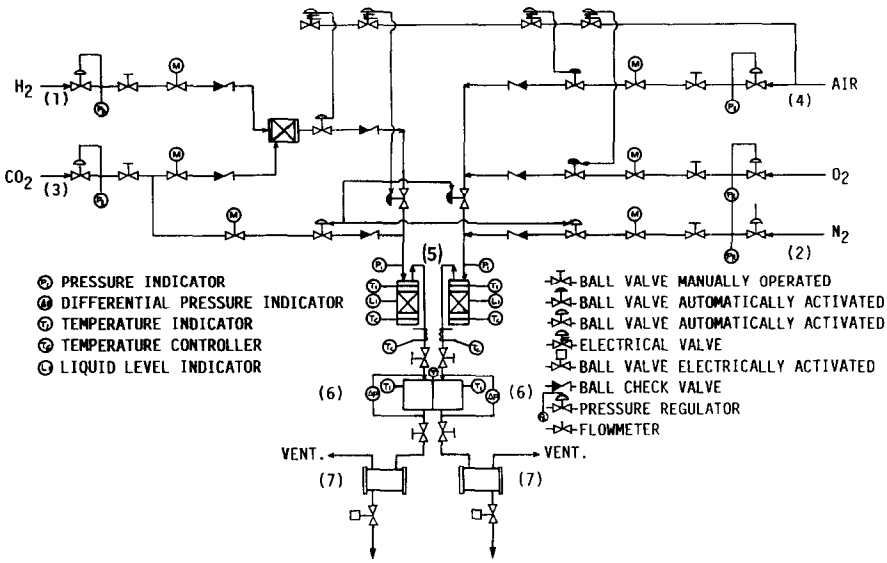

Fig. 1. Schematic diagram of the monocell plant.

ducers (6) measure and check the pressure on the anode and cathode. Two condensers (7) for the fuel and oxidant exhausts, respectively, are located outside of the monocell.

The monocell module uses graphite monopolar plates and internal gas collectors for the working gases to permit a more compact system and to simplify gas sealing. The upper (outlet) and lower (inlet) copper plates are the only external gas collectors, and a bracket and tie-rod system is used to seal the monocell. Each plate is provided with thermocouples and on the anode plate there is an acid reservoir connected through a Teflon tube to an external reservoir to supply continuously H_3PO_4 to the cell. The electrode area is 72 cm^2.

Cell components

The catalysts were prepared by a colloidal dispersion-based procedure described elsewhere [8]. Table 1 reports main catalyst characteristics.

The electrodes used in the monocell tests were manufactured by a screen-printing procedure described elsewhere [5].

Electrochemical characterization of the electrodes (anodic and cathodic polarization) was carried out in a half-cell apparatus [5] with 98% w/w phosphoric acid at 170 °C. The platinum surface area was determined by cyclic voltammetry at a sweep rate of 50 mV s^{-1}. The hydrogen adsorbed in the potential range of 0.05–0.4 V (versus RHE) on flooded electrodes (10% polytetrafluoroethylene (PTFE)) was measured in 50% w/w phosphoric acid at room temperature.

The matrices were prepared by screen-printing and rolling procedures. Two kinds of SiC powders (diameter: 7 and 1 μm) are mixed with an aqueous solution of PTFE (Dupont Teflon 30N, 61% w/w) and isopropyl alcohol (0.1 ml IPA per g SiC). In the

TABLE 1

Catalysts characteristics[a]

	Electrode	Catalyst	Platinum content (%)	MSA (CV) ($m^2\ g^{-1}$)	D_{Pt} (A)	Catalyst layer, thickness (cm)	Platinum loading (mg cm^{-2})
A	(c) 63-T46	Pt-K22	19.4	22	125	0.012	0.51
B	(c) 63-T113	Pt-K31	19.7	113	24	0.011	0.56
C	(c) 63-T31R	Pt-K80	13.7	110	26	0.006	0.31
D	(a) 68-T11	Pt-K35	9.7	103	27	0.015	0.37

[a] (c) cathode, (a) anode.

rolling procedure the SiC–PTFE mixture is dried at 70 °C for 24 h, and the ground powder heated at 150 °C for 15 min and laminated until a 0.3-mm thickness is obtained. In the screen-printing procedure the mixture is degassed under vacuum at room temperature for 10 s and the applied directly on the cathode. The matrix is then dried at 70 °C and sintered at 320 °C for 15 min. The final thickness of the matrix is 0.15 mm.

Testing methodology

Before assembling, the electrodes and the matrices have been pre-impregnated with purified 90% phosphoric acid at 130 °C in air for 48 h. The loss of carbon due to precorrosion effects was 0.11 mg cm^{-2}, equal to 1% of the catalytic layer.

The electrolyte was prepared by diluting purified reagent-grade H_3PO_4 (Carlo Erba, 99% w/w) with bidistilled water to a concentration of 90 wt.%. The purification procedure is described in ref. 4.

The cell was sealed by using the matrix and a film of PTFE as a gasket around the edge of the cathodic monopolar plate. This provided a good sealing with no risk of short-circuit in case the matrix developed a crack. A graphite paper (papiex 'N', Le Carbone–Lorraine) was employed to obtain adequate electrical conductivity between the graphite plates and the copper end plate. The overall voltage loss, due to the contact electrical resistance, was lower than 3 mV at 200 mA cm^{-2}.

The electrolyte, consumed during the test, was continuously fed in the cell through a channel located on the anodic monopolar plate filled with a paste made of carbon fibre and phosphoric acid, and communicating with an external reservoir.

All tests were performed with humidified hydrogen and dry air (utilization coefficients = 0.5 for both H_2 and air) which were preheated at 120 °C before entering the cell.

The internal resistance was measured by the current interruption technique using an oscilloscope (Philips PM 3305) connected to the cell and synchronized to the switch of the load.

X-ray photoelectron spectroscopy (XPS) spectra of the electrodes before and after the endurance tests were taken using an ESCA Lab 2000 spectrometer (Perking Elmer). Al Kα X-radiation was used at a power of 300 W and the analyser parameters were: pass energy 89.5 eV and at constant resolution.

Results and discussion

A series of runs, each lasting about 1000 h, has been planned to screen the effects of several operating parameters on the cell performance under continuous load conditions.

The evaluation included: (i) fuel humidifier temperature; (ii) cell working current, and (iii) phosphoric acid management.

Since the contribution of water flow diffusing through the matrix from the cathode to the anode is negligible (less than 1.2×10^{-6} mol min^{-1} cm^{-2}), mostly a function of the permeability of the electrodes and matrix [14], the water content at the anode is equivalent to the quantity of water in the H_2 gas passing through the humidifier. The results of the calculation of the water flow at a fixed H_2 flow rate ($U_F=0.5$ at 300 mA cm^{-2}) for different humidifier temperatures are given in Fig. 2. The corresponding phosphoric acid concentration in equilibrium with the water vapour pressure is also given.

The water balance at the cathode should be a function of the water from the humidifier and that produced via the electrochemical reaction. Due to the high content of water produced electrochemically (Fig. 3) at the stated working current densities (300–350 mA cm^{-2}), the air at the inlet of the cathode is not humidified. In Fig. 3, the corresponding changes in the concentration of phosphoric acid at a fixed air-flow rate ($U_0=0.5$ at 300 mA cm^{-2}) are also reported.

The concentration of the acid is a very important parameter in the cell operation, since high concentrations (>100%) result in low ionic conductivity [15] which affects the ionic resistance of the cell. On the contrary, at a concentration lower than 95%, an abrupt increase in carbon corrosion is to be expected [16]. A good compromise between these two parameters is achieved by operating in the range 98–99 wt.% acid. It means, as demonstrated in Fig. 3, that with dry air and a fixed air-flow rate, current densities as high as 300–350 mA cm^{-2} will maintain the phosphoric acid concentration

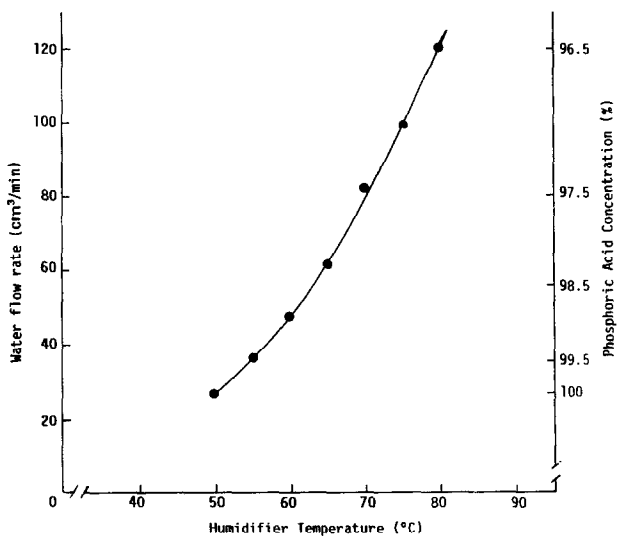

Fig. 2. Water-flow rate at the anode and phosphoric acid concentration at different humidifier temperatures; H_2 flow rate: 216 cm^3 min^{-1}; cell temperature: 180 °C.

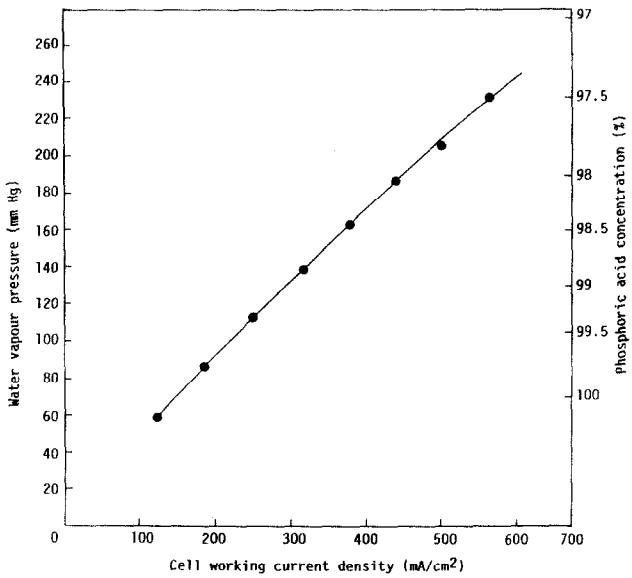

Fig. 3. Water-vapour pressure at the cathode and phosphoric acid concentration vs. cell current density; air flow rate: 750 cm^3 min^{-1}; cell temperature: 180 °C.

in the range indicated above. The corresponding humidifier temperature of H_2 should be in the range 60–70 °C. Under these conditions the power density becomes significant (~ 170 mW cm^{-2} at 350 mA cm^{-2}) and the lower cell voltages (0.5–0.55 V) are beneficial in decreasing the carbon corrosion and platinum sintering phenomenon, which are both enhanced at higher potentials.

Besides the change in acid concentration, another important factor which affects the cell performance is the loss of acid in the reactant gases or absorbed in the graphite plate. The losses depend on the cell temperature, gas-flow rate, and the phosphoric acid retention by the matrix. Since the temperature and gas-flow rates were kept constant in all runs, we have assumed that the factor which regulates the phosphoric acid flow from the cell is the capillary force (p) of the matrix:

$$p = \frac{2\gamma \cos \vartheta}{r} \tag{1}$$

where γ is the surface tension, ϑ is the contact angle and r is the capillary radius.

Assuming γ and ϑ are constant in components of different runs, the observed phosphoric acid losses were expected to be dependent only upon the porosity of the matrix. This was confirmed by the experimental data reported in Fig. 4 where the rapid increase of phosphoric acid losses is a linear function of the porosity of the matrix. These results are in good agreement with literature values [17] where a total loss of 1.26×10^{-5} cm^3 h^{-1} cm^{-2} of cell is reported to be distributed among the acid carried by the air flow (1.08×10^{-5} cm^3 h^{-1} cm^{-2}), that carried out by the H_2 flow (0.05×10^{-5} cm^3 h^{-1} cm^{-2}), and that adsorbed in the bipolar plates (0.13×10^{-5} cm^3 h^{-1} cm^{-2}).

The porosity and absorption properties of the matrix also affect the cell ionic resistance. According to Shiota [18] the ionic resistance of a matrix follows Bruggeman's equation [19]:

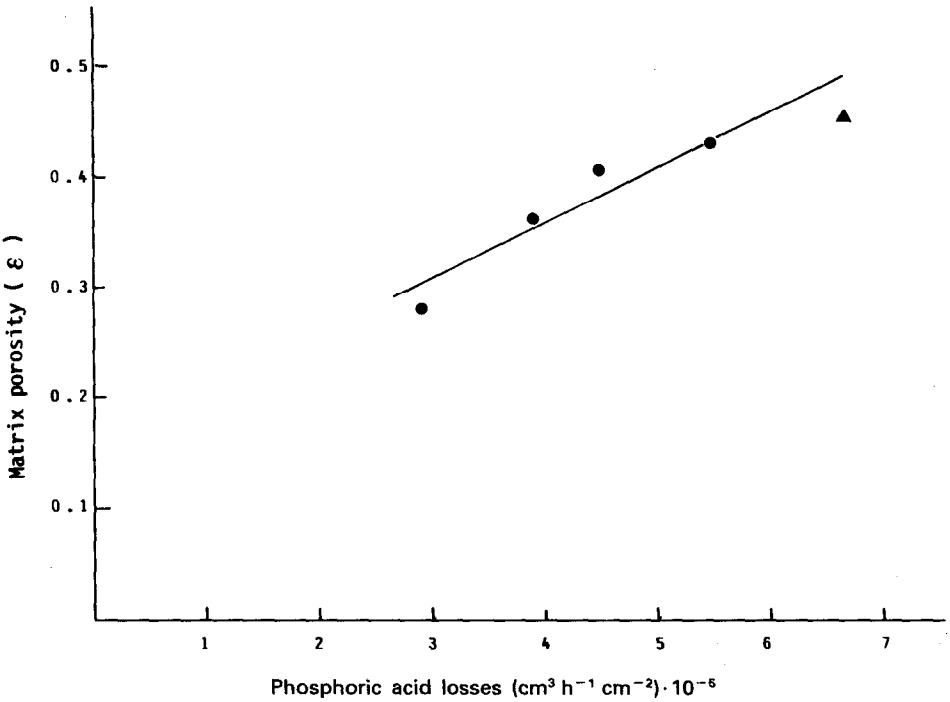

Fig. 4. Phosphoric acid losses during cell operation vs. matrix porosity: (●) rolling matrices, and (▲) screen-printing matrix.

$$R_{ion} = \frac{1}{K_L}\frac{1}{f}\frac{L}{S} \tag{2}$$

where K_L is the ionic conductivity of the acid equal to 0.59 Ω^{-1} cm^{-1} for 98% H_3PO_4 at 180°, L is the thickness of the matrix in cm, S is the geometric area in cm^2, and f is the 'effectiveness factor' (dimensionless), a function of the product of the porosity (ϵ) and the filling degree (β) of the matrix $f=(\epsilon\beta)^{3/2}$.

In Fig. 5 the variation of ionic resistivity is reported as a function of $\epsilon\beta$ for a series of runs made by varying the absorption/morphological properties of the matrices. Differences in the thickness are normalized in Fig. 5 by plotting R_{ion}/L versus $\epsilon\beta$.

Besides the study carried out on the cell-operating parameters, a second series of runs has been directed towards an extensive analysis on the effects of the characteristics of the catalyst and electrode on performance decay. Figure 6 shows the performance history of three typical runs with platinum–carbon cathodes made from different catalysts (Table 1). The run carried out with Pt-K31 cathode catalyst (MSA = 113 m^2 g^{-1}) showed the highest performance stability with a total voltage loss of 2.1 mV per 1000 h. In the first 1700 h with Pt-K22 (MSA = 22 m^2 g^{-1}), the voltage loss was of the same order, or even lower (1.5 mV per 1000 h), but it was followed by a rapid decay with a total voltage loss of 17.2 mV per 1000 h. Finally, the run with Pt-K80 (MSA = 110 m^2 g^{-1}) was extremely stable except for an abrupt (accidental) decay. A voltage loss of 2.0 mV per 1000 h was recorded under steady conditions.

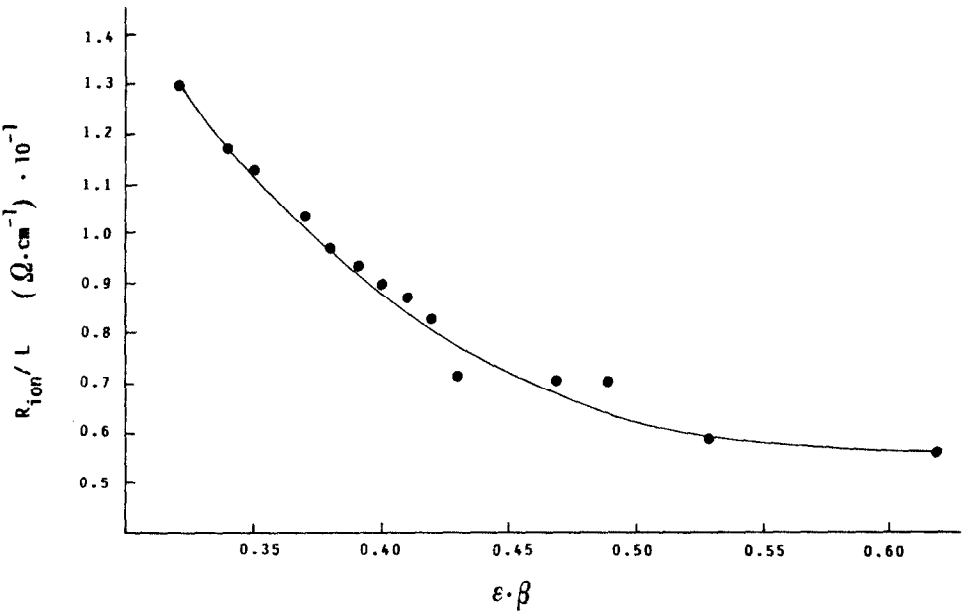

Fig. 5. Cell ionic resistance as a function of $\epsilon\beta$.

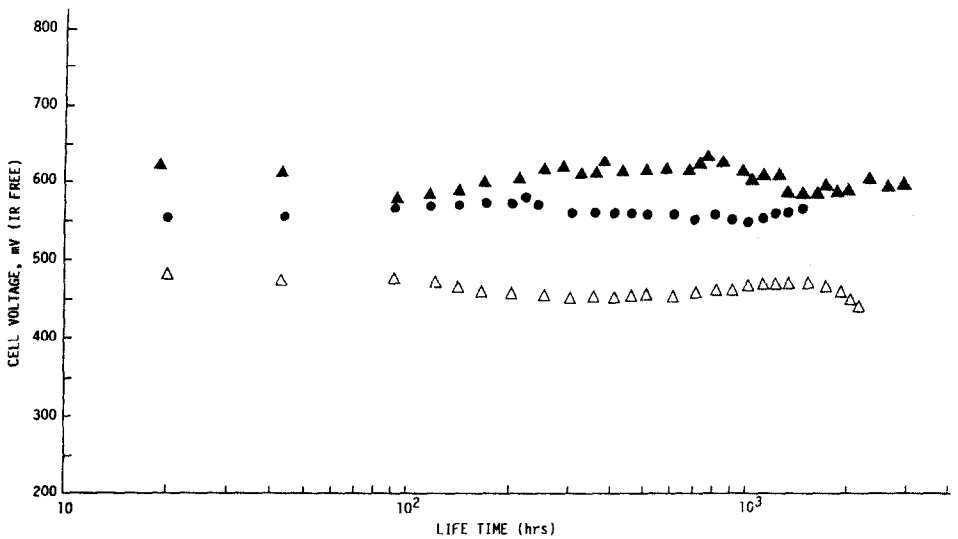

Fig. 6. Cell performance decay: (▲) cathode catalyst Pt-K80; (●) cathode catalyst Pt-K31; (△) cathode catalyst Pt-K22. Cell temperature: 180 °C; pressure 1 atm; fuel humidifier temperature: 60 °C; oxidant humidifier temperature: 25 °C; working current density: 250 mA cm^{-2}; fuel and air utilization coefficients: 0.5.

We have tried to explain this behaviour taking into account two prevailing mechanisms of decay, one related to the catalyst and the other to the electrode. The first, which is attributed to platinum sintering and dissolution, is known to occur from the very beginning of the runs and is driven by the tendence of the smaller platinum particles to dissolve in the acid by virtue of their greater surface energy. It has been demonstrated that the particle surface energy is inversely related to its radius [20] and hence the activity of platinum for dissolution should be greatest on the smallest particles which dissolve and recrystallize until larger more stable crystals are formed. The agglomeration is accelerated at high potentials and is especially rapid above 0.8 V versus RHE [21]. Working at lower voltages dramatically decreases the propensity to sintering and this explains the extremely low decay rates observed even if high surface area catalysts are considered. The cyclic voltammetry measurements made on the electrode prepared with Pt-K80 catalyst are in agreement with this interpretation as the platinum surface area retention after 48 h at constant current density (200 mA cm^{-2}) and at 0.7 V versus RHE was found to be nearly 100%.

Morphological modifications of the electrode structure, due to the preparative parameters (PTFE content, sintering temperature, etc.) play a big role especially in the long run [22]. Literature information on morphological modifications induced by long-term operation of PAFC electrodes is generally lacking. Klinedinst *et al.* [23] examined the effect of the potential variation on the stability of the PTFE–graphite interaction and measured the change in the rates of their separation in the presence of hot phosphoric acid. Jindra *et al.* [24] used XPS measurements to characterize some Ni–PTFE bond electrodes, and have interpreted a splitting of the F and C signals (from the Teflon), as a result of different qualities of contact between the Teflon and graphite particles. To this end and to clarify the influence of the structural changes of the electrodes on the performance stability, we have performed a series of XPS analysis before and after the test on the components of a 2000-h run (Pt-K22 cathode catalyst). The major peaks on the spectra were identified as F2s, Pt4f, Si2p, Si2s, C1s, O1s, F1s and F (KLL) Auger. The F signal originates from the surface-exposed Teflon. The Pt is a result of the catalyst at the surface. The Si is associated with the SiC in the matrix. The carbon gives two peaks at 285 and 292 eV due to carbon in the graphite and Teflon, respectively. The oxygen at the surface derives from the functional groups of the carbon and from the oxidized Pt species, and a clear distinction between the two contributions is not evident.

Analysis of our electrodes (Fig. 7) revealed that the most significant chemical changes after test are in the spectra of the C1s. The chemical identity of the peaks observed were interpreted following Wagner [25]. The peak at 283 eV is due to a carbide from SiC in the matrix. The peak at 284.5 eV is due to the graphitic carbon in the catalyst and to the carbon contamination at the surface originating from the laboratory environment. Three more peaks were identified between 286 and 290 eV, likely attributable to oxidized carbon that have one, two, three associated oxygens, respectively. The peak at about 292 eV is due to the carbon in Teflon and its high binding energies in the relation with the strong electron-withdrawing power of the fluorine. The effect of surface charging is quite evident also in the F1s spectra (Fig. 8). A big variation in the amount of Teflon at the cathode surface is noted after the test. This loss of Teflon can be correlated with the loss of adhesion of the PTFE–carbon interface in the electrode structure with depletion of the Teflon from the surface, according to a nonequilibrium process related to the effect of the electric potential. The decrease in adhesion is in fact observed at the cathode due to the

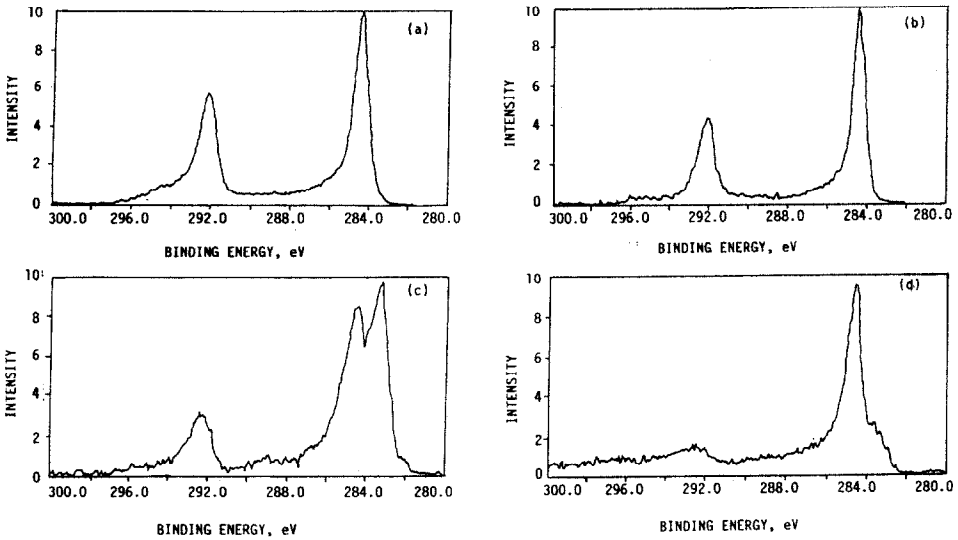

Fig. 7. XPS C1s spectra of the (a) anode before test; (b) anode after test; (c) cathode before test, and (d) cathode after test. Cathode catalyst Pt-K22.

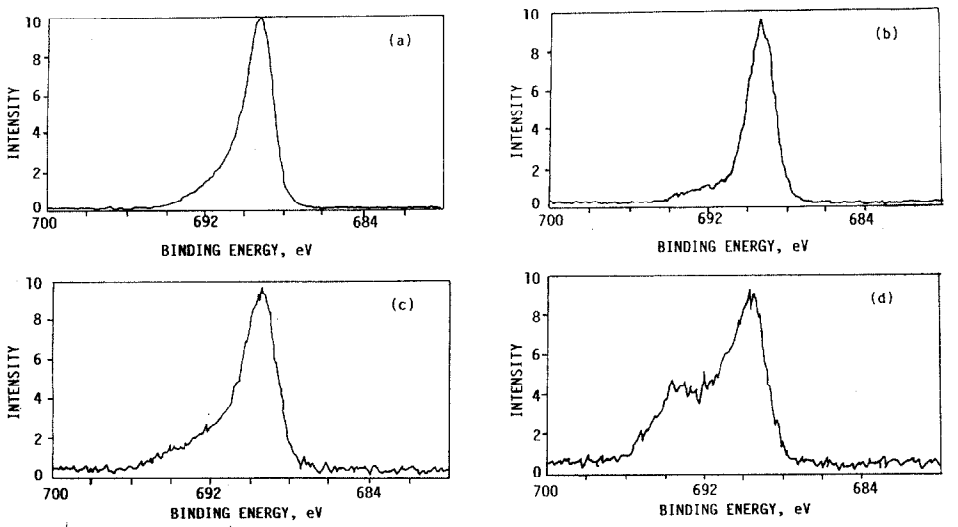

Fig. 8. XPS F1s spectra of the (a) anode before test; (b) anode after test; (c) cathode before test, and (d) cathode after test. Cathode catalyst Pt-K22.

larger operating potential (0.5–0.6 V) than that of the anode (0.1–0.3 V), in agreement with Klinedinst's results.

Modifications of the surface texture of the electrode materials cause an increase of the wetting properties of the catalytic structure and a progressive absorption of phosphoric acid. This condition yields in an increase of electrode polarization due to larger mass-transfer process, and explains the observed decrease of performance with the time.

Besides the above discussion, this paper also presents a brief illustration of the progress made at this Institute in improving the overall performance of a PAFC by research on the catalyst and the electrode morphology. With reference to catalysts A and B in Table 1, improvement in going from a low to a high surface catalyst is evident from comparison of their performances (Fig. 6). Although obvious, the gain in performance obtained by increasing the surface area of the catalyst is substantiated by extensive work carried out in our Institute [6, 8]. The bulk of our recent work has demonstrated not only a close correspondence between surface area and performance but it gave also a detailed interpretation of differences arising from adjustment in the preparation procedures and activation conditions of the electrodes. A careful control of the morphological properties, as illustrated in our previous works has allowed us to tailor-make electrodes of high activity with even lower platinum loadings resulting in a saving of platinum. Careful control of morphological properties coupled with an extensive check on the modelling behaviour of electrodes has made it possible to obtain electrodes that can operate at high current densities in the order of 350 mA cm^{-2}, which is a desirable goal for PAFC technology. Because of these adjustments, higher power densities were obtained that fit well with the requirements for an economical exploitation of the technology.

Conclusions

The subscale monocell tests allowed us to define the correct start-up and working conditions of the typical PAFC components developed by our Institute. Together with observations on the effects of ageing, important key parameters for the scaling up of our 1-kW PAFC unit have been derived.

The effect of voltages, current density, humidifier temperatures, and gas-flow rates on the cell performance have been carefully investigated and the optimum range of these parameters has been selected. The results point to a relationship among these variables and the phosphoric acid concentration which in turn controls the internal resistance of the cell and the kinetics of carbon corrosion. The latter process is an important parameter that has a strong influence on the life of the system.

Performance stability tests have indicated that the most predominant mechanism of decay of our electrode formulations is connected with the structural changes of electrode itself, and can be correlated with the loss of adhesion at the PTFE–carbon interface.

By careful control of the catalyst properties and the electrode morphological absorptive characteristics, power densities of 160–180 mW cm^{-2} have been attained in long-term operations, voltage decay being in the order of 2 mV per 1000 h. Research is in progress to consolidate and ameliorate these characteristics.

References

1 N. Itoh, *J. Power Sources, 29* (1990) 29.
2 N. Giordano, *Settimana Italo-Sovietica delle arti della scienza della cultura, Moscow, Oct. 12–22, 1989.*
3 P. Zegers, *Proc. Int. Fuel Cell Conf. (IFCC), Makuhari, Japan, Febr. 3–6, 1992,* pp. 17–20.
4 P. L. Antonucci, F. Romeo, M. Minutoli, V. Alderucci and N. Giordano, *Carbon, 26* (1988) 197.

5 N. Giordano, E. Passalacqua, L. Pino, A. S. Aricò, V. Antonucci, M. Vivaldi and K. Kinoshita, *Electrochim. Acta, 36* (1991) 1979.
6 N. Giordano, P. L. Antonucci, E. Passalacqua, L. Pino, A. S. Aricò and K. Kinoshita, *Electrochim. Acta, 36* (1991) 1931.
7 E. Passalacqua, P. L. Antonucci, M. Vivaldi, A. Patti, V. Antonucci, N. Giordano and K. Kinoshita, *Electrochim. Acta, 37* (1992) 2725.
8 N. Giordano, E. Passalacqua, P. L. Antonucci, L. Pino, M. Vivaldi, A. Patti and K. Kinoshita, *Electrochim. Acta,* in press.
9 N. Giordano, E. Passalacqua, V. Alderucci, P. Staiti, L. Pino, H. Mirzaian, E. J. Taylor and G. Wilemski, *Electrochim. Acta, 36* (1991) 1049.
10 V. Alderucci, E. Passalacqua, N. Giordano, P. L. Antonucci, F. Parmigiani and N. Ricci, *J. Appl. Electrochem., 20* (1990) 235.
11 N. Giordano, E. Passalacqua, V. Recupero, M. Vivaldi, E. J. Taylor and G. Wilemski, *Electrochim. Acta, 35* (1990) 1441.
12 K. Okano, *Proc. Int. Fuel Cell Conf. (IFCC), Makuhari, Japan, Febr. 3–6, 1992,* pp. 129–132.
13 J. H. Hirschenhofer, *Proc. 25th Intersociety Energy Conversion Engineering Conf. (IECEC), Reno, NV, USA, Aug. 12–17, 1990,* pp. 176–184.
14 T. Tsukui, personal communication.
15 Der-Tau Chin and H. H. Chang, *J. Appl. Electrochem., 19* (1988) 95.
16 P. Stonehart and J. P. Mac Donald, *EPRI EM-1664*, EPRI, Palo Alto, CA, USA, 1981.
17 T. Mori, A. Honji, T. Kahara and Y. Hishinuma, *J. Electrochem. Soc., 135* (1988) 1105.
18 H. Shiota, K. Mitsuda, J. Aragane and T. Murachashi, *Ext. Abstr., The Electrochemical Society Fall Meet., Hollywood, FL, USA, Oct. 15–20, 1989,* Abstr. No 88.
19 H. Voget, Gas-Evolving Electrodes, in E. Yeager *et al.* (eds.), *Comprehensive Treatise of Electrochemistry,* Plenum, New York, 1983.
20 K. Kinoshita, K. Routsis, J. A. S. Bett and C. S. Brooks, *Electrochim. Acta, 18* (1973) 953.
21 P. Bindra, S. J. Clouser and E. Yeager, *J. Electrochem. Soc., 126* (1979) 1631.
22 V. Alderucci, V. Recupero, E. Passalacqua, F. Parmigiani, D. L. Cocke and N. Giordano, *Bull. Electrochem., 7* (1991) 91.
23 K. A. Klinedinst and W. M. Vogel, *J. Adhes., 9* (1978) 123.
24 J. Jindra, I. Krejci, J. Mrha, B. Folkesson, L. Y. Johansson and R. Lasson, *J. Power Sources, 13* (1984) 123.
25 C. D. Wagner, W. M. Riggs, L. E. Davis and J. F. Moulder, in G. E. Muilenberg (ed.), *Handbook of X-ray Photoelectron Spectroscopy,* Perking-Elmer Corporation, Minnesota, 1978.